Confinement as a determinant of macromolecular structure and reactivity

Allen P. Minton

Laboratory of Biochemical Pharmacology, National Institute of Diabetes, Digestive and Kidney Diseases, National Institutes of Health, Bethesda, Maryland 20892 USA

ABSTRACT The confinement of macromolecules within enclosures or "pores" of comparable dimensions results in significant size- and shape-dependent alterations of macromolecular chemical potential and reactivity. Calculations of the magnitude of this effect for model particles of different shapes in model enclosures of different shapes were carried out using hard particle partition theory developed by Giddings et al. (*J. Phys. Chem.* 1968. 72:4397–4408). Results obtained indicate that the equilibrium constants of reactions, such as isomerization, self-association, and site binding, that result in significant change in macromolecular size, shape, and/or mobility may be altered within pores by as much as several orders of magnitude relative to the value in the unbounded or bulk phase. Confinement also produces a substantial size-dependent outward force on the walls of an enclosure. These results are likely to be important within the fluid phase of biological media, such as the cytoplasm of eukaryotic cells, containing significant volume fractions of large fibrous structures (e.g., the cytomatrix).

INTRODUCTION

The cytoplasm of almost all eukaryotic cells contains a variety of fibrous "supramolecular" structures, such as F-actin, microtubules, and intermediate filaments, collectively referred to as the cytomatrix, cytoskeleton, or microtrabecular lattice (Porter, 1984). It has been estimated from a three-dimensional analysis of electron micrographs that the total volume of fibrous elements is on the order of 20% of the total volume of cytoplasm (Gershon et al., 1985). A rough calculation based upon this figure suggests that most of the fluid phase of cytoplasm (that is, the part of cytoplasm exterior to the fibrous structures) lies within a few macromolecular radii of the surface of at least one fibrous structural element (Minton, 1990). Electron microscopic evidence (Hirokawa, 1991) also suggests that the fluid phase of cytoplasm is largely distributed in pores, interstices, and channels between fibrous structures. Fluorescence recovery after photobleaching (FRAP) and EPR studies (Mastro et al., 1984; Luby-Phelps et al., 1987) have revealed that the cytomatrix retards diffusive transport of soluble molecules within the cytoplasm in a size-dependent manner, with larger molecules being most significantly slowed. This work constitutes a first attempt to address the following questions. Can the confinement of soluble components of the cytoplasm within pores or channels alter the equilibrium (as opposed to transport) behavior of these components? If so, under what conditions would such alterations be significant?

In the following section the basic relations between equilibria in confined and unconfined phases are described and specified in terms of differential partitioning of reactants and products between the unconfined and confined phases. Next, general elements of partition theory (Giddings et al., 1968) are reviewed: calculations of partitioning for specific models are deferred to the appendix. Next, results of calculations of the effects of confinement upon isomerization, association, and binding equilibria in model enclosures ("pores") are presented. Then, some results are presented illustrating linkage between solution equilibria in pores and the ability of the system to perform mechanical work via expansion or compression. Finally, the possible biological relevance of the results presented are discussed.

RELATIONS BETWEEN EQUILIBRIA IN UNCONFINED AND CONFINED PHASES

Consider the following general reaction in solution:

$$n_1X_1 + n_2X_2 + \cdots + n_jX_j \rightleftarrows n_{j+1}X_{j+1} + n_{j+2}X_{j+2} + \cdots + n_NX_N.$$

A thermodynamic equilibrium association constant for this reaction at fixed temperature and pressure is defined in molar concentration units as follows:

$$K_0 \equiv \prod_{i=j+1}^{N} a_i^{n_i} \Big/ \prod_{i=1}^{j} a_i^{n_i} = \prod_{i=j+1}^{N} c_i^{n_i}\gamma_i^{n_i} \Big/ \prod_{i=1}^{j} c_i^{n_i}\gamma_i^{n_i}, \quad (1)$$

where a_i, c_i, and γ_i denote respectively the (molar) thermodynamic activity, molar concentration, and (molar) activity coefficient of the ith species. We may also define apparent equilibrium constants for the unbounded ("bulk") and bounded ("pore") phases in terms of the concentrations of each species within the respective phase:

$$K^{\text{bulk}} \equiv \prod_{i=j+1}^{N} (c_i^{\text{bulk}})^{n_i} \Big/ \prod_{i=1}^{j} (c_i^{\text{bulk}})^{n_i} \quad (2)$$

$$K^{\text{pore}} \equiv \prod_{i=j+1}^{N} (c_i^{\text{pore}})^{n_i} \Big/ \prod_{i=1}^{j} (c_i^{\text{pore}})^{n_i}, \quad (3)$$

where the superscript denotes the phase to which the corresponding variable refers. Assuming equilibrium be-

0006-3495/92/10/1090/11 $2.00

tween bulk and pore phases, then $a_i^{\text{pore}} = a_i^{\text{bulk}}$ for all i, and

$$K^{\text{pore}} = K^{\text{bulk}}\Gamma, \tag{4}$$

where

$$\Gamma \equiv \prod_{i=j+1}^{N} (\gamma_i^{\text{bulk}}/\gamma_i^{\text{pore}})^{n_i} \Big/ \prod_{i=1}^{j} (\gamma_i^{\text{bulk}}/\gamma_i^{\text{pore}})^{n_i}.$$

We next define an equilibrium partition coefficient for the ith species as follows:

$$\mathcal{K}_i \equiv c_i^{\text{pore}}/c_i^{\text{bulk}} = \gamma_i^{\text{bulk}}/\gamma_i^{\text{pore}}. \tag{5}$$

Thus, Eq. 4 may be rewritten as:

$$K^{\text{pore}}/K^{\text{bulk}} = \Gamma = \prod_{i=j+1}^{N} \mathcal{K}_i^{n_i} \Big/ \prod_{i=1}^{j} \mathcal{K}_i^{n_i}. \tag{6}$$

The excess free energy of confinement is defined as the free energy change associated with the transfer of one mole of macrosolute from the bulk phase to the confined phase under standard state conditions:

$$\begin{aligned}\Delta G_{\text{conf},i} &\equiv \mu_i^{\text{pore}} - \mu_i^{\text{bulk}} \\ &= RT \ln (\gamma_i^{\text{pore}}/\gamma_i^{\text{bulk}}) = -RT \ln \mathcal{K}_i.\end{aligned} \tag{7}$$

It follows from Eqs. 6 and 7 that:

$$RT \ln \Gamma = \sum_{i=1}^{j} n_i \Delta G_{\text{conf},i} - \sum_{i=j+1}^{n} n_i \Delta G_{\text{conf},i}. \tag{8}$$

Thus, reaction equilibria will be shifted to the right if the free energy cost of confining products is less than that of confining reactants, and shifted to the left if the cost of confining products is greater than that of confining reactants.

In the following section the calculation of partition coefficients is described, and it is shown that value of a particular partition coefficient $\mathcal{K}_i$ depends upon the size and shape of a molecule of species i relative to the size and shape of the confining pore. When the partition coefficient of each reactant and product has been determined, the ratio of equilibrium constants characterizing the overall reaction in the pore and bulk phases is calculated via Eq. 6.

PARTITION THEORY FOR CONFINED VOLUMES OF UNIFORM SIZE

Giddings et al. (1968) developed a statistical theory for the equilibrium partitioning of rigid molecules into inert porous networks. Results of that theory used in the present study are summarized below.

Let $U(r, \phi)$ denote the potential energy of interaction between a rigid body and the surface of a confining volume, defined as a function of the position of its center of mass, denoted by the vector variable r, and its orientation, denoted by the vector variable ϕ. For the present, we neglect interactions between solute molecules in the fluid phase. Under such conditions it was shown by Giddings et al. (1968) that the ratio of the concentration of a rigid body within a confined volume element to that of the same rigid body within an unconfined element of equal size and shape is given by the ratio of configurational integrals in the two phases:

$$\mathcal{K} = \frac{\int\int \exp[-U(\phi, r)/kT]\, d\phi\, dr}{\int\int d\phi\, dr}. \tag{9}$$

The exponential vanishes in the denominator because the potential energy of interaction with boundaries is defined to be zero for all positions and orientations in the bulk phase. Depending upon the details of the particular particle and pore shapes selected, it may be preferable to evaluate the double integrals by first integrating with respect to position and then with respect to orientation, or vice-versa. Thus, the position-dependent micropartition coefficient $\kappa(r)$ and the orientation-dependent micropartition coefficient $\kappa'(\phi)$ are defined as follows:

$$\kappa(r^*) \equiv \frac{\int \exp[-U(\phi, r^*)/kT]\, d\phi}{\int d\phi} \tag{10}$$

$$\kappa'(\phi^*) \equiv \frac{\int \exp[-U(\phi^*, r)/kT]\, dr}{\int dr}. \tag{11}$$

It follows from Eqs. 9–11 that:

$$\mathcal{K} = \frac{\int \kappa(r)\, dr}{\int dr} = \frac{\int \kappa'(\phi)\, d\phi}{\int d\phi}. \tag{12}$$

Although Eq. 9 is completely general, in this work we shall neglect long range interactions between solute and confining surfaces and consider only the hard particle model, in which $U(r, \phi) = 0$ when the particle does not intersect the surface, and $U(r, \phi) = \infty$ when the particle intersects the surface. Thus each point in configuration space $\{r, \phi\}$ is associated with an exponential term or weighting factor of either 1 or 0, depending upon whether that configuration is nonintersecting (physically allowed) or intersecting (physically disallowed). In this fashion the problem of evaluating partition coefficients is reduced to the simpler geometric problem of evaluating volumes in the space of allowed configurations.

In this work we model solute species as rigid particles of one of four different shapes, illustrated in Fig. 1. These particles are fully described in the appendix. (*a*) A globular protein or a globular aggregate of protein subunits is modeled as a sphere or cube. For spherical or cubical hard particles, the partition coefficient is simply the ratio

of the volume within an enclosure accessible to the center of the particle (termed "available volume") to the total volume of the enclosure. (*b*) A rodlike protein or a rodlike aggregate of protein subunits is modeled as a spherocylinder. The configurational integral for a spherocylinder in a regularly shaped pore is equal to that of a rod of infinitesimal thickness with length equal to that of the spherocylinder minus twice the radius, in a pore of identical shape but with surfaces displaced normally inward by a distance equal to the radius of the spherocylinder (Giddings et al., 1968). The partition coefficient is reasonably simply evaluated for the pore geometries considered in this work (see appendix). (*c*) A disklike protein or a disklike aggregate of protein subunits is modeled as a spherodisk. The configurational integral for a spherodisk in a regularly shaped pore is equal to that of a disk of infinitesimal thickness with radius equal to that of the spherodisk minus half its thickness, in a pore of identical shape but with surfaces displaced normally inward by a distance equal to half of the thickness of the spherodisk (Giddings et al., 1968). The partition coefficient is reasonably simply evaluated for the cases of a spherodisk between two parallel planes and within a spherical cavity (see appendix).

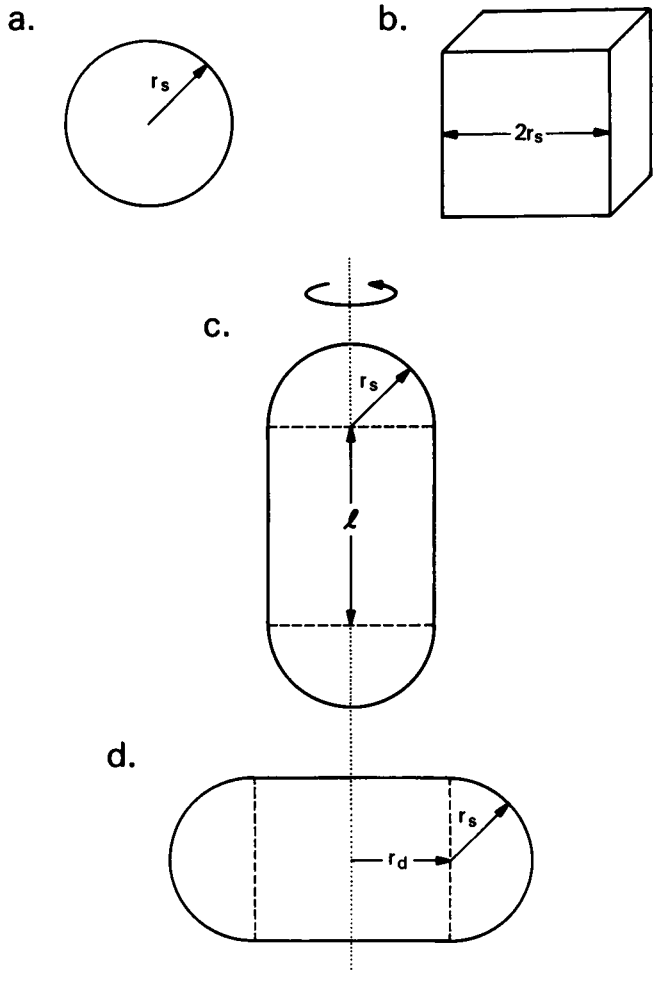

FIGURE 1 Model particles used for calculation of partition coefficients; full specification in part I of the appendix.

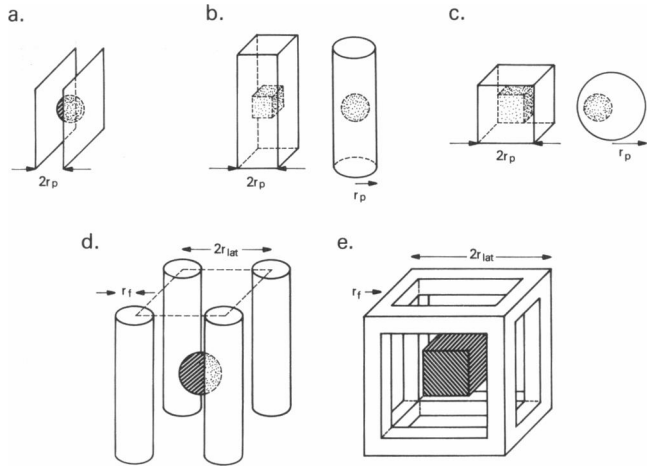

FIGURE 2 Model enclosures or "pores" used for calculation of partition coefficients; full specification in part II of the appendix. Shaded bodies are examples of enclosed particles.

In this work we model elements of confined volume by several model enclosures, illustrated in Fig. 2. These enclosures are fully described in the appendix. A volume bounded by two parallel planes, called a planar pore, is used as a model for confinement in one dimension. A cylindrical pore is used as a model for confinement in two dimensions, and a spherical or cubical cavity is used as a model for confinement in three dimensions. Some results are also presented for a spherical solute in the interstices between aligned cylindrical rods and for a cubical solute between intersecting rods of square cross-section in a cubical lattice.

RESULTS AND DISCUSSION

Isomerization equilibria

The effect of confinement upon the tendency of a solute particle (single polypeptide chain or oligomer of fixed composition) to adopt a particular shape[1] is reflected in the relative magnitudes of ΔG_{conf} calculated for differently shaped particles of equal volume in pores of equal dimension. Values of ΔG_{conf} for three different particle shapes (spherical, spherodiscoidal, and spherocylindrical) are plotted as functions of relative pore size for planar, cylindrical, and spherical pores in Fig. 3, *a–c*.

[1] By the term "shape," we mean the conformation of the molecule at low resolution: quasi-spherical, rod-like, disk-like, etc.

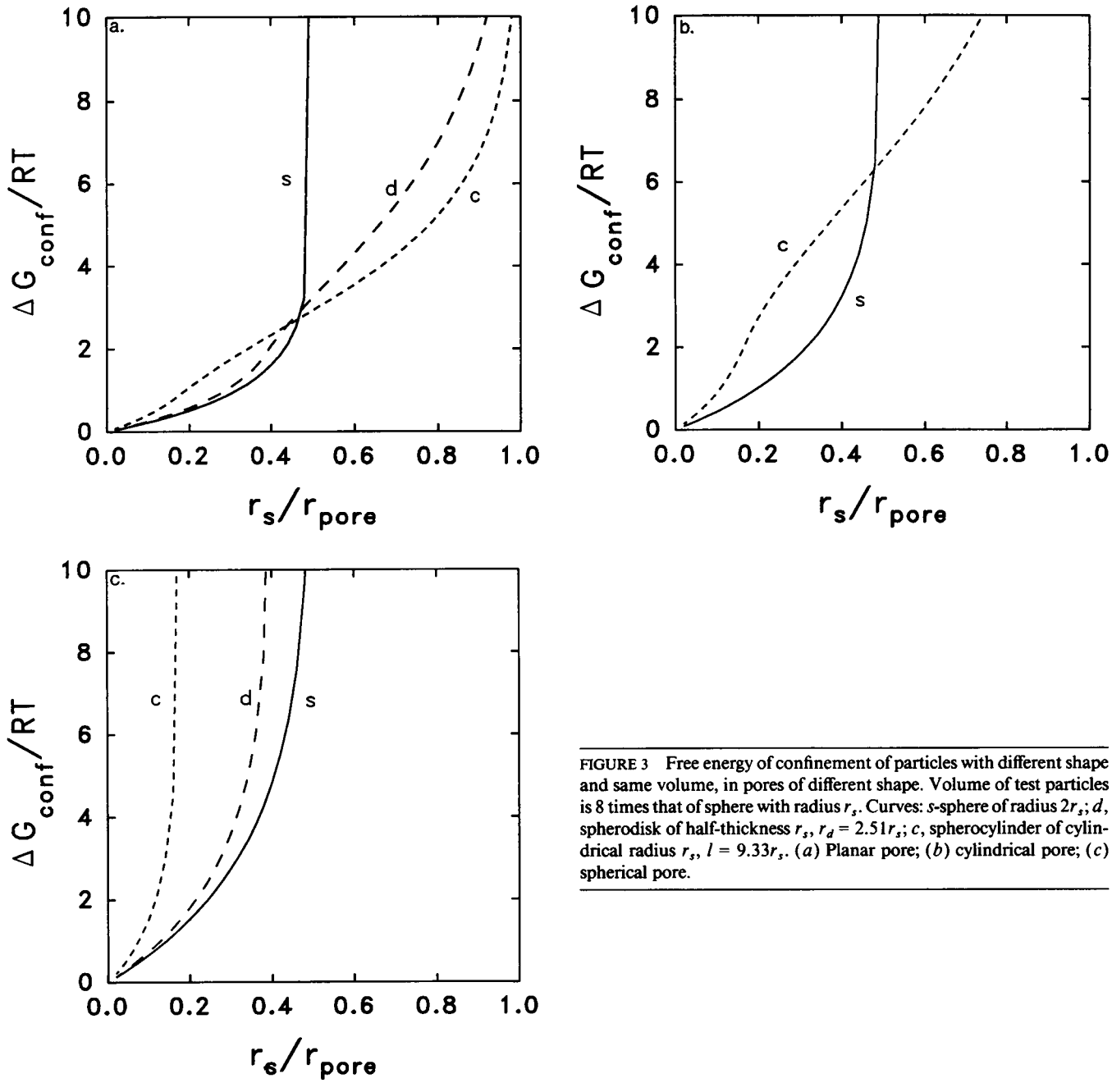

FIGURE 3 Free energy of confinement of particles with different shape and same volume, in pores of different shape. Volume of test particles is 8 times that of sphere with radius r_s. Curves: *s*-sphere of radius $2r_s$; *d*, spherodisk of half-thickness r_s, $r_d = 2.51r_s$; *c*, spherocylinder of cylindrical radius r_s, $l = 9.33r_s$. (*a*) Planar pore; (*b*) cylindrical pore; (*c*) spherical pore.

The results shown indicate that as the dimension of a particle approaches the spacing of confining boundaries, (*a*) the free energy cost of confinement rises substantially, and (*b*) becomes increasingly dependent upon particle shape for fixed particle volume. Spherical particles, which are the most compact for a given volume, have the lowest free energy cost of confinement and are hence most favored in larger pores (low values of r_s/r_{pore}). However, spherical particles are totally excluded from cylindrical or planar pores that may be occupied by rodlike or discoidal particles of equal volume. We note that the behavior of the discoidal particle falls between that of the spherical and rodlike particle in both planar and spherical pores, and, interestingly, while not optimal in either environment, seems to be only marginally suboptimal in both environments.

Monomer-*n*mer association

For the simple equilibrium $nA \rightleftarrows A_n$, Eq. 6 reduces to:

$$\Gamma = \mathcal{K}_n/\mathcal{K}_1^n, \tag{13}$$

where $\mathcal{K}_i$ denotes the partition coefficient of *i*-mer. The value of Γ was calculated for the self association of spherical monomers to form dimers, tetramers, octamers, and hexadecimers having spherical, rodlike, and disklike shapes of equal volume in planar, cylindrical, and spherical pores, and is plotted as a function of relative pore size

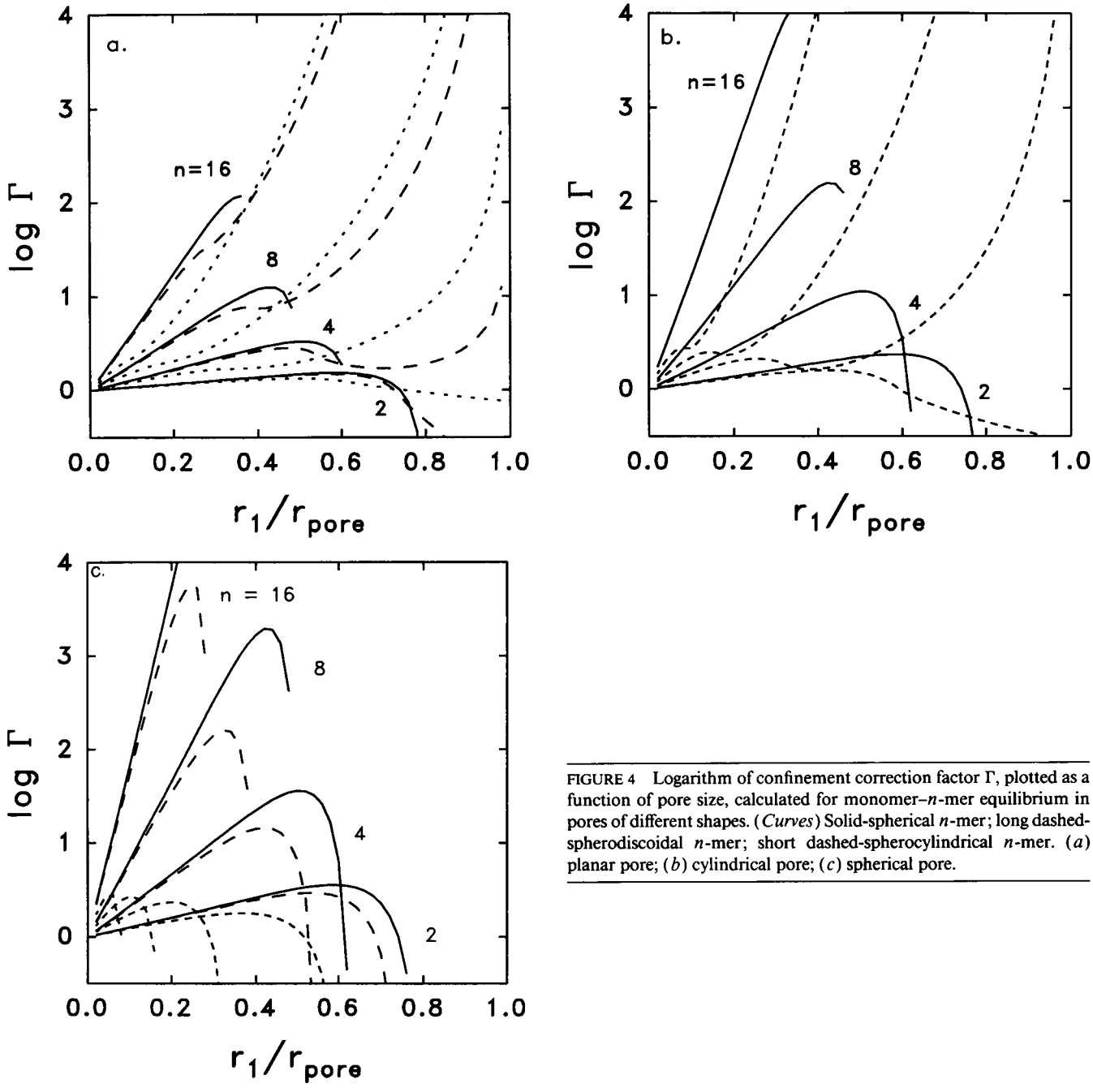

FIGURE 4 Logarithm of confinement correction factor Γ, plotted as a function of pore size, calculated for monomer–n-mer equilibrium in pores of different shapes. (*Curves*) Solid-spherical n-mer; long dashed-spherodiscoidal n-mer; short dashed-spherocylindrical n-mer. (*a*) planar pore; (*b*) cylindrical pore; (*c*) spherical pore.

in Fig. 4, *a–c*. The value of Γ was also calculated for the self association of cubical monomers to form cubical dimers, tetramers, octamers and hexadecimers in a cubical lattice of parallelopiped fibers, and is plotted as a function of the ratio of monomer size to lattice spacing in Fig. 5.

The results show that confinement can enhance the tendency of compact particles to self associate by as much as several orders of magnitude, and that the degree of enhancement depends upon the sizes and shapes of both the resulting oligomer and the bounded volume element. Formation of globular aggregates is favored when the geometry of the enclosure permits accommodation of the globular aggregate.

Indefinite isoenthalpic self association to a linear oligomer

Consider the following indefinite self association reaction:

$$A + A \rightleftarrows A_2 \qquad K_2 \equiv c_2/c_1^2$$
$$A_2 + A \rightleftarrows A_3 \qquad K_3 \equiv c_3/c_2c_1$$
$$\cdots$$
$$A_{n-1} + A \rightleftarrows A_n \qquad K_n \equiv c_n/c_{n-1}c_1,$$

where c_i represents the molar concentration of i-mer. It has been shown that when identical monomers self associate to form oligomers in an ideal (unbounded) solu-

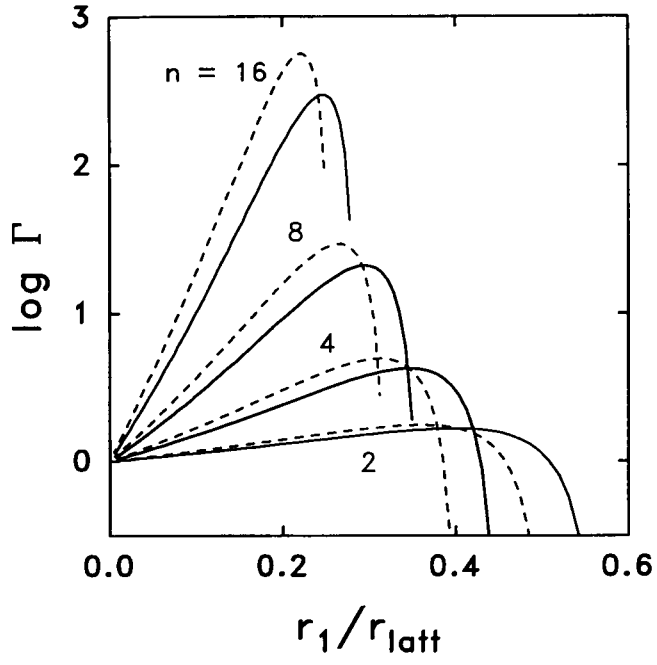

FIGURE 5 Logarithm of confinement correction factor Γ, plotted as a function of lattice spacing, calculated for cubical monomer-cubical n-mer equilibrium in a cubic lattice of parallelopiped fibers. Fractional occupancy of total volume by fibers: 0.2 (*solid curves*) and 0.3 (*dashed curves*).

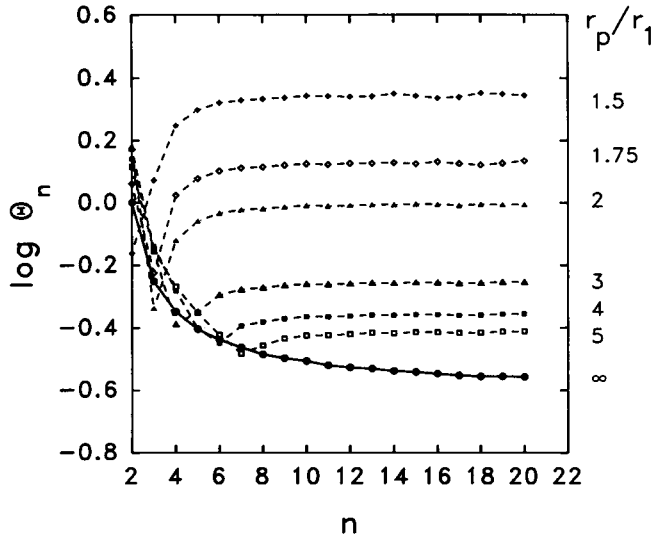

FIGURE 6 Logarithm of Θ_n plotted as a function of n, calculated for cylindrical pores of several different sizes. Points plotted for $r_p/r_1 = \infty$ represent values taken from Chatelier (1987).

tion, the standard state entropy changes associated with the addition of successive monomers to a growing oligomer depend upon the size and shape of the oligomer (Hill and Chen, 1973; Chatelier, 1987). When the enthalpy change associated with monomer addition is independent of oligomer size (isoenthalpic self association), the free energy change associated with successive additions increases with the extent of association, resulting in diminishing values of K_i as i increases (Chatelier, 1987).

Let us define the ratio $\mathcal{R}_n \equiv K_n^{\text{bulk}}/K_2^{\text{bulk}}$, the value of which may be calculated approximately using relations presented by Chatelier (1987). It follows from Eq. 6 that

$$\Theta_n \equiv \frac{K_n^{\text{pore}}}{K_2^{\text{bulk}}} = \frac{K_n^{\text{pore}}}{K_n^{\text{bulk}}} \times \mathcal{R}_n = \frac{\mathcal{K}_n}{\mathcal{K}_{n-1}\mathcal{K}_1} \times \mathcal{R}_n. \qquad (14)$$

We have calculated the value of Θ_n for a model in which spherical monomers associate isoenthalpically to form linear oligomers represented as spherocylinders with radius r_1 and length determined by conservation of volume, within a cylindrical pore. Results are presented as a function of n for pores of varying radii in Fig. 6.

The major qualitative result observed is that whereas Θ_n decreases with increasing n in the bulk (or in large pores), it increases with n for sufficiently small pore dimensions. The significance of this result is illustrated in the following example. Using Eq. 14, the fraction of total solute mass present as n-mer in an equilibrium mixture of oligomers ($1 \leq n \leq 20$) was calculated as a function of pore size for a macrosolute with $K_2^{\text{bulk}} = 1\ \mu\text{M}^{-1}$ and total concentration of protomers = 45 μM. The results shown in Fig. 7 indicate that the equilibrium distribution of oligomers in a cylindrical pore becomes extremely sensitive to changes in pore dimension as the radius of the pore decreases below $\sim 3r_1$.

Binding of a soluble ligand to surface sites

Consider a simple equilibrium between a mobile ligand species A and a stationary independent binding site on the surface of a fiber:

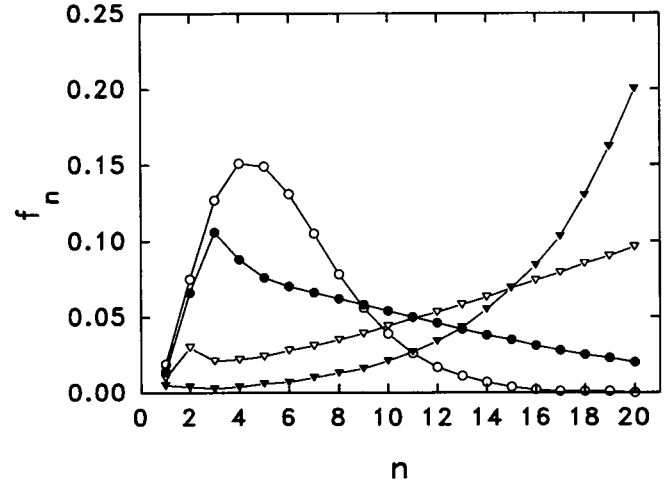

FIGURE 7 Mass fraction of n-mer at equilibrium, plotted as a function of n for a reversibly oligomerizing solute in a cylindrical pore. Points calculated as described in the text for $r_p/r_1 = \infty$ (*hollow circles*), 3 (*filled circles*), 2 (*hollow triangles*), and 1.5 (*filled triangles*).

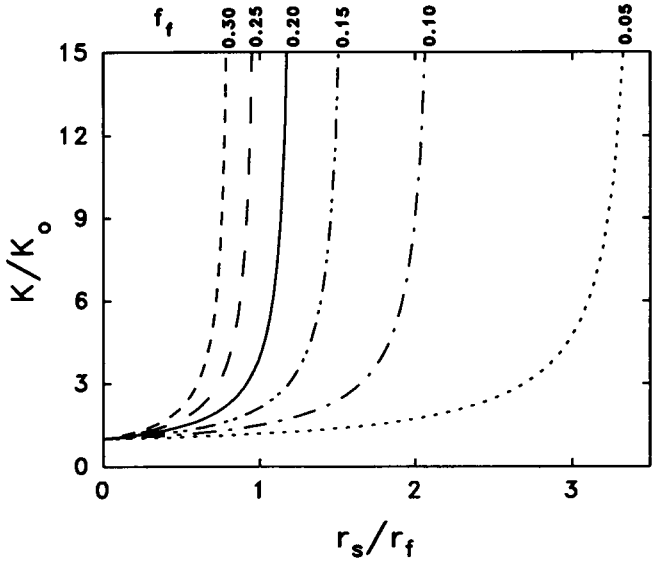

FIGURE 8 Effect of ligand size upon site binding constant in square lattice of aligned cylindrical fibers, calculated for several different values of f_f, the fractional occupancy of lattice volume by fibers.

$$[A] + \text{site} \rightleftarrows [A]\cdot\text{site},$$

with association equilibrium constant K_0 in the bulk. For this system the number of ligands bound is given as a function of the concentration of free ligand by the Langmuir isotherm (Tanford, 1961):

$$n_{\text{bound}} = y \times n_{\text{sites}}, \tag{15a}$$

where

$$y = \frac{K_0 a}{1 + K_0 a} = \frac{Kc}{1 + Kc}, \tag{15b}$$

where a and c are, respectively, the thermodynamic activity and concentration of free ligand, and

$$K = K_0\gamma = K_0/\mathcal{H}, \tag{15c}$$

where γ and $\mathcal{H}$ are respectively the activity and partition coefficients of free ligand. The dependence of K upon the ratio of ligand to fiber diameter in a square array of aligned cylindrical fibers is plotted for several different volume fractions of fiber in Fig. 8. Of particular interest is the sharp dependence of binding constant upon ligand size as the size of the ligand approaches the characteristic spacing of the array. When the fractional extent of site occupancy is small ($y \ll 1$), then y, and hence n_{bound}, will increase linearly with K for constant c.

"Sealed" versus "open" pores

Many of the results presented above were calculated assuming that the concentration of solute within a pore remains constant as the dimensions of the pore change. Since the activity coefficient of the solute varies with pore dimensions, this will be true only to the extent that the fluid phase exists entirely within an environment of uniformly sized pores. If solute within a pore is allowed to equilibrate with bulk (unconfined) solute, or with solute in larger pores, then the equilibrium concentration of solute within the (smaller) pores will decrease as the dimensions of the pore shrink. An illustration of this effect follows.

Consider a solute that may exist as an equilibrium mixture of spherical monomer and linear (spherocylindrical) octomer. The equilibrium constant sufficient to provide a weight fraction of 50% oligomer in an ideal solution at a total concentration of 1 g/liter is calculated to be 128 $(\text{liter/g})^{-7}$. If a bulk solution containing 1 g/liter of solute is equilibrated with planar pores having dimensions large relative to that of the solute, then both monomer and octamer will partition equally between bulk solution and pore. As the spacing of the planar pore diminishes, octamer will be preferentially excluded from the pore, leading to both a lowering of the total concentration of solute within the pore and a lowering of the weight fraction of solute within the pore existing as octamer. The magnitude of this effect is plotted in Fig. 9. Also shown in this figure is the contrasting behavior observed when the pore is sealed; if the solute cannot re-equilibrate with bulk solute as the pore dimensions di-

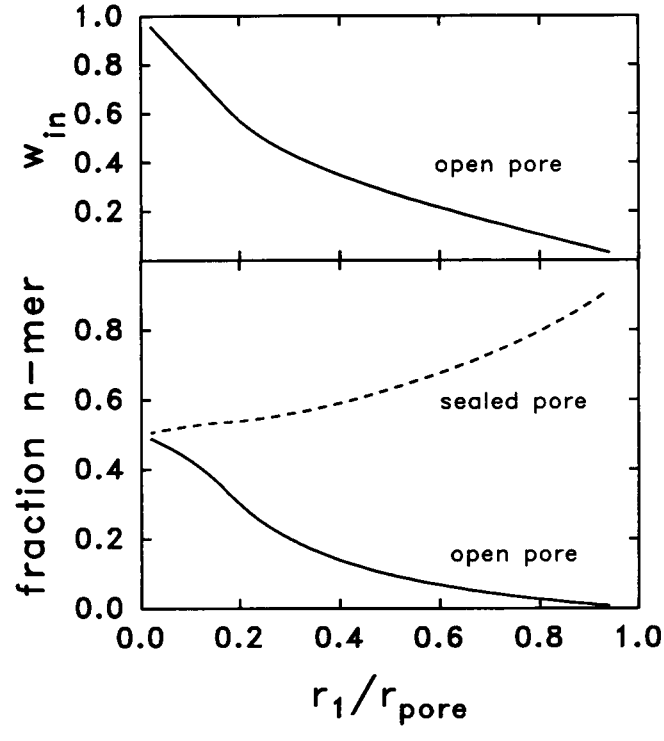

FIGURE 9 Effect of pore size upon distribution of a self associating macromolecule between unbounded solution and planar pores (*upper*) and upon state of association of macromolecule within the pore (*lower*). w_{in} is the total concentration of macrosolute in the pore, in equilibrium with a bulk concentration of 1 g/liter in the bulk phase.

minish, the extent of oligomerization within the pore increases (see above).

Eukaryotic cytoplasm is likely to contain microstructures corresponding to both open and sealed pores. The interstitial space between large fibrous elements of the cytomatrix may be regarded as an ensemble of open pores characterized by a possibly time-dependent distribution of sizes and shapes, while any microscopic region enveloped by membranes might be regarded as a sealed pore.

Mechanochemical linkage

Since the free energy of confined solutes is a function of pore dimensions, it follows that in a sealed pore, confined solutes exert force on the confining boundaries, and work may be performed if the boundaries are movable. In the case of an ideal solution confined between planar boundaries, the outward-directed force per mole of solute species i is given by:

$$f_i = -\frac{d\mu_i}{dl} = -\frac{1}{2}\frac{d\mu_i}{dr_p}, \tag{16}$$

where l is the distance between planar boundaries. According to Eq. 5, $\mathcal{K}_i\gamma_i^{pore} = \gamma_i^{bulk}$ (assumed here = 1). Hence $\mu_i = \mu_i^0 + RT\ln c_i - RT\ln \mathcal{K}_i$. It follows that when the volume of solution is held constant as r_p changes (by, for example, allowing the cross-sectional area of the enclosure to change),

$$f_i = \frac{RT}{2}\frac{d\ln \mathcal{K}_i}{dr_p}. \tag{17}$$

However, when the volume of solution increases linearly with r_p (by holding the cross-section constant and permitting the boundaries to be permeable to solvent), then

$$f_i = \frac{RT}{2}\left\{\frac{1}{r_p} + \frac{d\ln \mathcal{K}_i}{dr_p}\right\}. \tag{18}$$

The first term in the bracket on the right hand side of Eq. 18 results from macrosolute dilution with increasing r_p. The second term represents the contribution of confinement to the force exerted per mole of the ith component. The total force exerted by the solution is:

$$F \equiv \sum n_i f_i, \tag{19}$$

where n_i is the number of moles of the ith solute species between the planar boundaries.

The force exerted per mole of spherical macrosolute against the walls of a semi-permeable[2] planar enclosure is calculated from Eqs. 18 and (A1) to be:

[2] A semi-permeable enclosure permits solvent, but not macrosolutes, to pass through the enclosure boundaries.

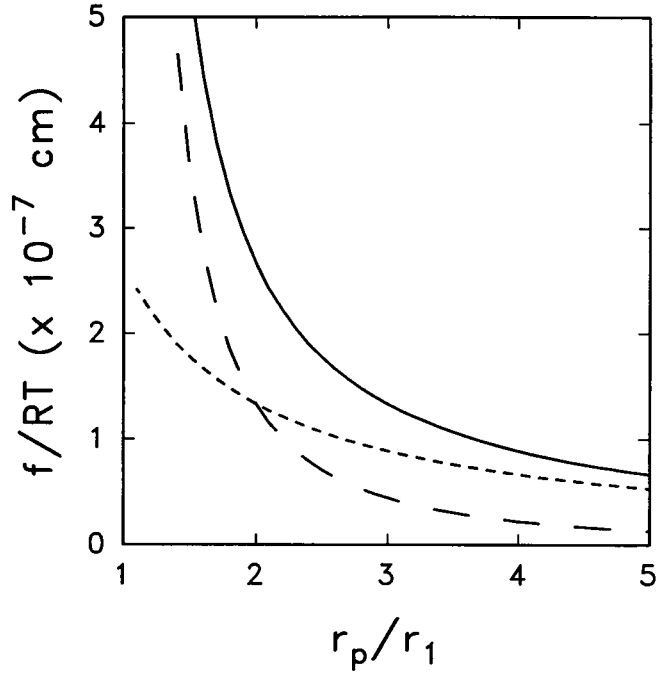

FIGURE 10 Effect of pore size upon the force exerted by spherical ligand against the semipermeable walls of a planar pore. The solid curve is the total force, and the short dashed curve and long dashed curve represent the contributions to the total force due to dilution and confinement effects respectively.

$$f_i = \frac{RT}{2}\left\{\frac{1}{r_p} + \frac{r_i}{r_p(r_p - r_i)}\right\}. \tag{20}$$

In Fig. 10, the force exerted per mole of monomer is plotted as a function of r_p. For small pore spacings ($r_p < 2r_1$) the force exerted by solute on the planar boundaries of the pore is dominated by the confinement effect (long dashed curve), and for large pore spacings ($r_p > 3r_1$) the force, which is substantially smaller in magnitude, is dominated by the ideal dilution effect (short dashed curve).

The force exerted by macrosolute may be modulated by altering the state of association, as illustrated in the following example. Consider a solute that may exist either as a globular (spherical) monomer of radius r_1 or as a globular octamer of radius $2r_1$ in reversible equilibrium with monomer, with $K_8^{bulk} \equiv w_8^{bulk}/(w_1^{bulk})^8$. The dependence of force upon equilibrium association constant is calculated as follows. For specified values of K_8^{bulk} and r_p, the value of K_8^{pore} is calculated using Eq. 13. Then the values of w_1 and w_8 are calculated subject to the constraint $w_{tot} = w_1 + w_8 = 1$. Finally, F, the total force exerted on the boundaries by monomer and octamer, is calculated using Eq. 19 and 20. F is plotted against the value of log K_8^{bulk} for four pore sizes in Fig. 11. It follows from the results shown in this figure that a change in solution conditions that substantially alters the value of K_8^{bulk} (such as addition of a specific small-molecule li-

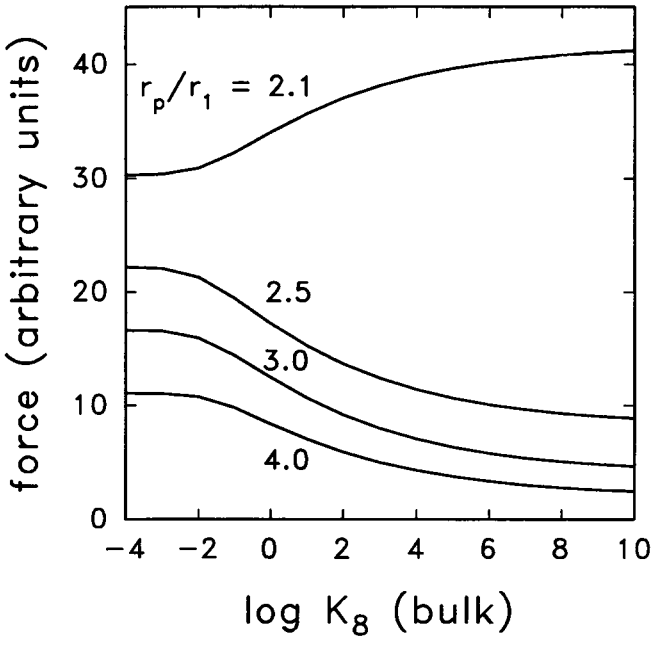

FIGURE 11 Effect of alteration in bulk equilibrium constant for octamerization upon the force exerted on the semipermeable walls of a planar pore, calculated for pores of several different sizes.

gand known to influence macromolecular self association) can result in significant increases or decreases in the force exerted by the solution upon the confining boundaries. If the boundaries are movable and the forces on opposite sides of a boundary become unbalanced, then large scale structural changes could conceivably be caused by ligand-linked association (or dissociation) of soluble globular proteins not ordinarily considered part of the structural apparatus of the cell.

POSSIBLE BIOLOGICAL RELEVANCE OF CONFINEMENT EFFECTS

The results presented here demonstrate that confinement of macromolecular solutes within bounded elements of fluid volume (pores, channels, interstices) can significantly affect the chemical potential and reactivity of those species whose largest dimension is within roughly a factor of three of the smallest characteristic spacing of the enclosure. Depending upon the relative shapes and sizes of the enclosure and the various solute species, confinement effects can result in substantial changes in isomerization, association, and surface binding equilibria relative to the bulk (unbounded) phase.

Confinement effects are similar in some respects to effects due to macromolecular crowding, that is, effects arising from volume exclusion in solutions of high total macromolecular content (Minton, 1981, 1983). Both crowding and confinement tend to enhance associations. However, while crowding always favors the formation of compact globular aggregates, confinement in one- or two-dimensional enclosures can sometimes favor the formation of extended (linear or discoidal) aggregates.

Microscopic studies reveal that the distribution of fibrous elements within the cytoplasm of a single cell can vary considerably from point to point (Bershadsky and Vasiliev, 1988). As this work suggests a significant linkage between cytomatrix structure and macromolecular equilibria in the intervening fluid phase, it is likely that inhomogeneities in fiber structure reflect corresponding inhomogeneities in solution phase chemistry as well. To the extent that increasingly sophisticated techniques of light and electron microscopy will permit point-to-point mapping of variations of local cytomatrix structure within the cell, relations of the type developed here may permit the construction of a corresponding map of the distribution of soluble macromolecules and their various states of association within the fluid phase of cytoplasm.

One of the major accomplishments of modern biochemistry has been to demonstrate how macromolecular association reactions in solution give rise to many of the large fibrous structures observed in the cytoplasm of living cells. Hopefully, this work will draw attention to the reciprocal influence of supramolecular structure upon solution biochemistry in cytoplasm and comparable biological environments.

APPENDIX

Partition coefficients for hard particles in variously shaped enclosures ("pores")

I. Specifications of model hard particles (Fig. 1)

(*a*) *Sphere.* Radius r_s; volume $V_s = 4\pi r_s^3/3$.

(*b*) *Cube.* Side $2r_s$; volume $V_c = 8r_s^3$. For the sake of simplicity in computation, the cube is constrained to orientations such that cube faces are either parallel or perpendicular to the plane surfaces bounding the enclosure.

(*c*) *Spherocylinder.* The volume obtained by rotating the area indicated in Fig. 1 *c* about the vertical axis; volume $V_{sc} = 4\pi r_s^3/3 + \pi r_s^2 l$.

(*d*) *Spherodisc.* The volume obtained by rotating the area indicated in Fig. 1 *d* about the vertical axis; volume $V_{sd} = 2\pi r_d^2 r_s + \pi^2 r_d r_s^2 + 4\pi r_s^3/3$.

II. Specifications of model enclosures (Fig. 2)

(*a*) *Planar pore.* Two parallel planes normal to the x axis located at $x = \pm r_p$.

(*b*) *Square parallelopiped pore.* An indefinitely long parallelopiped, the central axis of which is coincident with the z axis, having a square cross-section with sides at $x = \pm r_p$ and $y = \pm r_p$.

Cylindrical pore. An indefinitely long cylinder about the z axis, with radius r_p.

(*c*) *Cubical pore.* A cubical box centered at the origin, with sides at $x = \pm r_p$, $y = \pm r_p$, and $z = \pm r_p$.

Spherical pore. A spherical enclosure centered at the origin, with radius r_s.

(*d*) *Square array of parallel cylinders.* Fibers are modeled by cylinders of radius r_f, the axes of which are parallel to the z axis. Fiber axes pass through a square array of points in the $x - y$ plane with a nearest neighbor distance of $2r_{lat}$.

(*e*) *Cubical lattice of parallelopipeds.* A three-dimensional net-

work of fibers modeled by indefinitely long parallelopipeds extending in three perpendicular directions (parallel to the x, y, and z axes). Three mutually perpendicular fibers intersect at each point in a cubical lattice of points, with nearest neighbor intersections occurring at intervals of $2r_{lat}$ in the x, y, and z directions. Each fiber has a square cross-section, with side $2r_f$.

III. Calculation of partition coefficients

(*a*) *No orientation factor.* In the case of a cube with orientation constrained as specified above, or a sphere, the partition coefficient is simply the ratio of the volume accessible to the center of the particle to the volume accessible to a point particle.

(*b*) *Orientation factor.* In the case of a spherocylinder or spherodisk, partition coefficients are calculated in two stages. For planar or spherical enclosures, an expression for the position-dependent micropartition coefficient $\kappa(r)$ is obtained by evaluating the fraction of allowed orientations for a fixed position (Eq. 10). This expression is subsequently integrated over all positions to obtain $\mathcal{K}$ (Eq. 12). For the case of a spherocylinder in a cylindrical enclosure, an expression for the orientation-dependent micropartition coefficient $\kappa'(\phi)$ is obtained by evaluating the fraction of allowed positions for a fixed orientation (Eq. 11). This expression is subsequently integrated over all orientations to obtain $\mathcal{K}$ (Eq. 12).

IV. Partition coefficients for various models

1. Planar pore

(*a*) *Spherical or cubic particle.* The center of mass of an enclosed sphere may be located at any position (x, y, z), such that $|x| \le (r_p - r_s)$. The partition coefficient is given by the ratio of allowed to total pore volumes:

$$\mathcal{K} = 1 - \alpha, \tag{A1}$$

where $\alpha \equiv r_s/r_p$. The same equation holds for an enclosed cube if the cube is constrained orientationally as described above.

(*b*) *Spherocylindrical particle.* Let $r'_p \equiv r_p - r_s$ and $q \equiv r_l/r'_p$. Then

$$\kappa(r) = \begin{cases} 1 & r < (r'_p - r_s) \\ \dfrac{r_p - r}{r_l} & r \ge (r'_p - r_s) \end{cases} \tag{A2}$$

$$\mathcal{K} = \frac{1}{r_p}\int_0^{r_p} \kappa(r)\,dr = \begin{cases} 1 - q/2 & r_l < r'_p \\ 1/(2q) & r_l \ge r'_p. \end{cases} \tag{A3}$$

(*c*) *Spherodiscoidal particle.* Let $q \equiv r_d/r'_p$. Then

$$\kappa(r) = \begin{cases} 1 & r < (r'_p - r_s) \\ 1 - \sqrt{1 - \left(\dfrac{r'_p - r}{r_d}\right)^2} & r \ge (r'_p - r_s) \end{cases} \tag{A4}$$

$$\mathcal{K} = \frac{1}{r_p}\int_0^{r_p} \kappa(r)\,dr = \begin{cases} \dfrac{r'_p}{r_p}\cdot\left(1 - \dfrac{\pi}{4}q\right) & r_d < r'_p \\ \dfrac{r'_p}{r_p}\cdot\left(1 - \dfrac{1}{2}\sqrt{1 - q^{-2}} - \dfrac{q}{2}\sin^{-1}(q)\right) & r_d \ge r'_p. \end{cases} \tag{A5}$$

2. Cylindrical pore

(*a*) *Spherical particle.* The center of mass of the sphere may lie at any position (r, z) such that $0 \le r \le (r_p - r_s)$. The partition coefficient, equal to the ratio of allowed to total volumes, is given by:

$$\mathcal{K} = (1 - \alpha)^2, \tag{A6}$$

where $\alpha \equiv r_s/r_p$. This result is identical to that obtained in the case of an orientationally constrained cube enclosed in a parallelopiped of square cross-section.

(*b*) *Spherocylindrical particle.*

$$\kappa'(\theta) = \begin{cases} \displaystyle\int_0^{r'_p - r_l\sin\theta} \sqrt{r'^2_p - (x + r_l\sin\theta)^2}\,dx & (r'_p - r_l\sin\theta) > 0 \\ 0 & (r'_p - r_l\sin\theta) \le 0 \end{cases} \tag{A6}$$

$$\mathcal{K} = \frac{4}{\pi r_p^2}\int_0^{\pi/2} \kappa'(\theta)\sin\theta\,d\theta. \tag{A7}$$

The integral expressions for $\kappa'(\theta)$ and $\mathcal{K}$ are evaluated via numerical quadrature.

3. Spherical pore

(*a*) *Spherical particle.* The center of mass of the sphere may lie at any point such that $r < (r_p - r_s)$. The partition coefficient, equal to the ratio of available to total volumes, is given by

$$\mathcal{K} = (1 - \alpha)^3, \tag{A8}$$

where $\alpha \equiv r_s/r_p$. The same equation holds for a cube in a cubical pore if the cube is constrained orientationally as described above.

(*b*) *Spherocylindrical particle.*

$$\kappa(r) = \begin{cases} 1 & r \le (r'_p - r_l) \\ \dfrac{r'^2_p - r_l^2 - r^2}{2rr_l} & (r'_p - r_l) < r < \sqrt{r'^2_p - r_l^2} \\ 0 & r \ge \sqrt{r'^2_p - r_l^2} \end{cases} \tag{A9}$$

$$\mathcal{K} = \frac{3}{r_p^3}\int_0^{r_p} \kappa(r)r^2\,dr = \frac{(r'_p - r_l)^3 + {}^3/_2 r_l(r'_p - r_l)^2}{r'^3_p}. \tag{A10}$$

(*c*) *Spherodiscoidal particle.* Let $q \equiv r_d/r'_p$. Then

$$\kappa(r) = \begin{cases} 1 & r \le (r'_p - r_d) \\ 1 - \dfrac{\sqrt{4r_d^2r^2 - (r'^2_p - r_d^2 - r^2)^2}}{2rr_d} & (r'_p - r_d) < r < \sqrt{r'^2_p - r_d^2} \\ 0 & r \ge \sqrt{r'^2_p - r_d^2} \end{cases} \tag{A11}$$

$$\mathcal{K} = \frac{3}{r_p^3}\int_0^{r_p} \kappa(r)r^2\,dr = \left(\frac{r'_p}{r_p}\right)^3 \times \left((1 - q^2)^{3/2} + \frac{3}{2}q^2(1 - q^2)^{1/2} - \frac{3}{2}q\sin^{-1}(q)\right). \tag{A12}$$

4. Aligned fibers

(*a*) *Cube in square array of parallelopipeds.* The volume available to an enclosed cube with orientation constrained as described above will be proportional to an area $r_{lat}^2 - (r_f + r_c)^2$; hence

$$\mathcal{K} = \frac{r_{lat}^2 - (r_f + r_c)^2}{r_{lat}^2 - r_f^2}. \quad \text{(A13)}$$

(*b*) *Sphere in square array of cylinders.* The volume available to an enclosed sphere of radius r_p is proportional to the cross-sectional area in the *xy* plane available to a circle of the same radius. By virtue of symmetry, one need consider only a quadrant of the square. The area available to a sphere of radius 0, i.e., a point, within this quadrant is $A_{point} = r_{lat}^2 - \pi r_f^2/4$. The area available to a sphere of finite radius, and hence the partition coefficient, depends upon the radius of the sphere:

case a: $0 \le (r_s + r_f) \le r_{lat}$:

$$\mathcal{K} = \{r_{lat}^2 - \pi(r_s + r_f)^2/4\}/A_{point} \quad \text{(A14)}$$

case b: $r_{lat} \le (r_s + r_f) \le \sqrt{2}r_{lat}$

$$\mathcal{K} = \left\{r_{lat}^2 - r_{lat}\sqrt{(r_c + r_f)^2 - r_{lat}^2} - \left(\frac{\pi}{4} - \Theta\right)(r_c + r_f)^2\right\}\Big/A_{point}$$

where

$$\Theta \equiv \cos^{-1}\left(\frac{r_{lat}}{r_c + r_f}\right). \quad \text{(A15)}$$

(*c*) *Cube in cubical lattice of parallelopiped fibers.* The volume available to a cube of side $2r_c$ will be proportional to $r_{lat}^3 - 3r_{lat}(r_f + r_c)^2 + 2(r_f + r_c)^3$; hence

$$\mathcal{K} = \frac{r_{lat}^3 - 3r_{lat}(r_f + r_c)^2 + 2(r_f + r_c)^3}{r_{lat}^3 - 3r_{lat}r_f^2 + 2r_f^3}. \quad \text{(A16)}$$

The author thanks Steven Zimmerman, William Eaton, and Dan Sackett for reviewing the initial draft of this report.

Received for publication 13 April 1992.

REFERENCES

Bershadsky, A. D., and J. M. Vasiliev, 1988. Cytoskeleton. Plenum Publishing Corp., New York.

Chatelier, R. C. 1987. Indefinite isoenthalpic self-association of solute molecules. *Biophys. Chem.* 28:121–128.

Gershon, N. D., K. R. Porter, and B. L. Trus. 1985. The cytoplasmic matrix: its volume and surface area, and the diffusion of molecules through it. *Proc. Natl. Acad. Sci. USA.* 82:5030–5034.

Giddings, J. C., E. Kucera, C. P. Russell, and M. N. Myers. 1968. Statistical theory for the equilibrium distribution of rigid molecules in inert porous networks. Exclusion chromatography. *J. Phys. Chem.* 72:4397–4408.

Hill, T. L., and Y.-D. Chen. 1973. Theory of aggregation in solution. I. General equations and application to the stacking of bases, nucleotides, etc. *Biopolymers.* 12:1285–1312.

Hirokawa, N. 1991. Molecular architecture and dynamics of the neuronal cytoskeleton. *In* The Neuronal Cytoskeleton. R. D. Burgoyne, editor. Wiley-Liss, New York. 5–74.

Luby-Phelps, K., P. E. Castle, D. L. Taylor, and F. Lanni. 1987. Hindered diffusion of inert tracer particles in the cytoplasm of mouse 3T3 cells. *Proc. Natl. Acad. Sci. USA.* 84:4910–4913.

Mastro, A. M., M. A. Babich, W. D. Taylor, and A. D. Keith. 1984. Diffusion of a small molecule in the cytoplasm of mammalian cells. *Proc. Natl. Acad. Sci. USA.* 81:3414–3418.

Minton, A. P. 1981. Excluded volume as a determinant of macromolecular structure and reactivity. *Biopolymers.* 20:2093–2120.

Minton, A. P. 1983. The effect of volume occupancy upon the thermodynamic activity of proteins: some biochemical consequences. *Mol. Cell. Biochem.* 55:119–140.

Minton, A. P. 1990. Holobiochemistry: an integrated approach to the understanding of biochemical mechanism that emerges from the study of proteins and protein associations in volume-occupied solutions. *In* Structural and Organizational Aspects of Metabolic Regulation. P. A. Srere, M. E. Jones, and C. K. Mathews, editors. Wiley-Liss, New York. 291–306.

Porter, K. R., editor. 1984. The cytoplasmic matrix and the integration of cellular function: proceedings of a conference. *J. Cell. Biol.* Vol. 99.

Tanford, C. 1961. Physical Chemistry of Macromolecules. John Wiley and Sons, Inc., New York.